Generalized Coupled Dielectric Waveguide and Its Variants for Millimeter-Wave Applications

A. K. TIWARI, BHARATHI BHAT, SENIOR MEMBER, IEEE, AND R. P. SINGH

Abstract—**The characteristic equations of hybrid TM and TE modes for a generalized coupled dielectric waveguide are derived using the mode-matching technique. From the characteristic equations of the generalized coupled dielectric waveguide, the phase constant, wave impedance, and field distribution can be evaluated. A variety of single and coupled dielectric waveguides can be obtained by assigning proper parameter values to the generalized coupled dielectric waveguide.**

I. Introduction

THE use of dielectric waveguides at millimeter-wave frequencies has been increasing for integrated circuits at millimeter-wave frequencies [1]–[11]. A number of dielectric waveguides such as the image guide [2], insular image guide [1], inverted strip dielectric waveguide, and trapped image guide have been reported using the effective dielectric constant method. Other structures which are of practical importance but have not been analyzed are the following:

1) shielded suspended single and coupled guide;
2) insulated broadside single and coupled dielectric guide;
3) insulated coupled nonradiative dielectric guide; and
4) insulated trapped coupled dielectric guide.

These can be derived from the generalized coupled dielectric waveguide configuration shown in Fig. 1.

The characteristics of a single dielectric guide structure are the same as those of a corresponding generalized coupled dielectric guide structure in the odd-mode excitation. The single dielectric guide structure therefore can be one-half of the coupled dielectric guide with an electric wall at the plane of symmetry in the direction of propagation.

II. Analysis

For the purpose of analysis, a generalized coupled dielectric guide structure is considered as shown in Fig. 1. Since the mode-matching technique is known to be more

Manuscript received September 30, 1985; revised March 27, 1986.

A. K. Tiwari and R. P. Singh are with the Department of Electronics Engineering, Maulana Azad College of Technology, Bhopal-462007, India.

B. Bhat is with the Centre for Applied Research in Electronics, Indian Institute of Technology, New Delhi-110016, India.

IEEE Log Number 8609061.

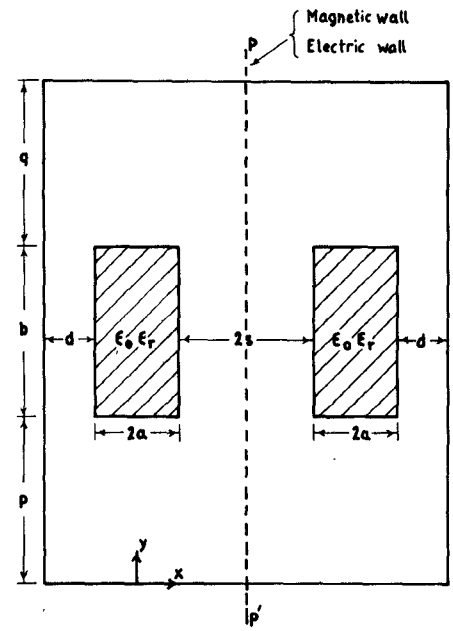

Fig. 1. Cross-sectional view of generalized dielectric waveguide structure.

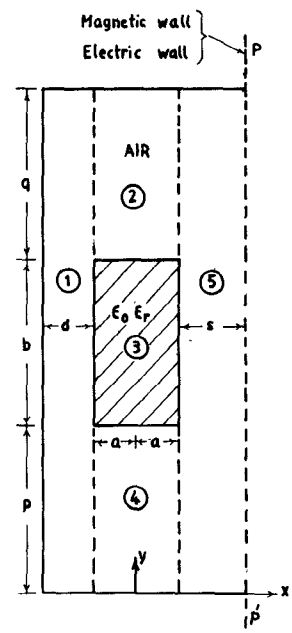

Fig. 2. Cross-sectional half-portion of the generalized dielectric waveguide for calculation of field distribution.

rigorous and accurate as compared to the effective dielectric constant method, the former method is used to analyze the above structure. The parameters p, q, b, $2a$, d, and s can be varied for different types of dielectric guide structures. In view of the symmetry of the generalized coupled dielectric guide structure to the plane pp', the analysis can be carried out in terms of even and odd modes. To facilitate the calculation of the electromagnetic fields in the transverse plane, the field region is subdivided into five parts as shown in Fig. 2. In such a structure, fields in any direction can be taken as a combination of TM and TE fields in that direction [16]. Here the modes in the generalized coupled dielectric guide will have all components of the E and H fields. The modes are classified TM and TE with respect to the y direction. For TM and TE modes, the electric and magnetic field components can be expressed in terms of a scalar potential function (given in the Appendix).

The various wavenumbers are related in the following manner:

$$\begin{aligned}
\beta_0^2 &= \beta_{1xm}^2 + \beta_{1ym}^2 + \beta^2 \\
&= \bar{\beta}_{1xn}^2 + \bar{\beta}_{1yn}^2 + \beta^2 \\
\beta_0^2 &= \beta_{2xm}^2 + \beta_{2ym}^2 + \beta^2 \\
&= \bar{\beta}_{2xn}^2 + \bar{\beta}_{2yn}^2 + \beta^2 \\
\beta_0^2 &= \beta_{3xm}^2 + \beta_{3ym}^2 + \beta^2 \\
&= \bar{\beta}_{3xn}^2 + \bar{\beta}_{3yn}^2 + \beta^2 \\
\beta_0^2 &= \beta_{4xm}^2 + \beta_{4ym}^2 + \beta^2 \\
&= \bar{\beta}_{4xn}^2 + \bar{\beta}_{4yn}^2 + \beta^2 \\
\beta_0^2 &= \beta_{5xm}^2 + \beta_{5ym}^2 + \beta^2 \\
&= \bar{\beta}_{5xn}^2 + \bar{\beta}_{5yn}^2 + \beta^2 \qquad (1)
\end{aligned}$$

where β_{1ym}, β_{2ym}, β_{3ym}, β_{4ym}, and β_{5ym} are the wavenumbers of TM mode of Regions I to V, respectively, in the y direction, and when the suffix y is replaced by x we get wavenumbers in the x direction. Further, $\bar{\beta}_{1yn}$, $\bar{\beta}_{2yn}$, $\bar{\beta}_{3yn}$, $\bar{\beta}_{4yn}$, and $\bar{\beta}_{5yn}$ are the wavenumbers in the y direction for the TE mode, and when the suffix y is replaced by x, we get the wavenumber in the x direction. Applying the boundary conditions at $y = 0$ and $y = p + b + q$,

$$\begin{aligned}
\beta_{1ym} = \beta_{5ym} &= \frac{m\pi}{p+b+q} \qquad m = 0,1,2,\cdots \\
\bar{\beta}_{1yn} = \bar{\beta}_{5yn} &= \frac{n\pi}{p+b+q} \qquad n = 1,2,3,\cdots . \qquad (2)
\end{aligned}$$

Matching the tangential field components E_z, H_z, E_x, H_x at $y = p$ and $y = p + b$, we get the transcendental equations for TM and TE modes in the y direction as reported elsewhere [4]. Further, matching the tangential field components E_y, E_z, H_y, H_z at $x = a$ over the range $0 \leqslant y \leqslant p$, $p \leqslant y \leqslant p + b$ and $p + b \leqslant y \leqslant p + b + q$ and using the principle of orthogonality, the value of the propagation constant in the direction of propagation can be computed.

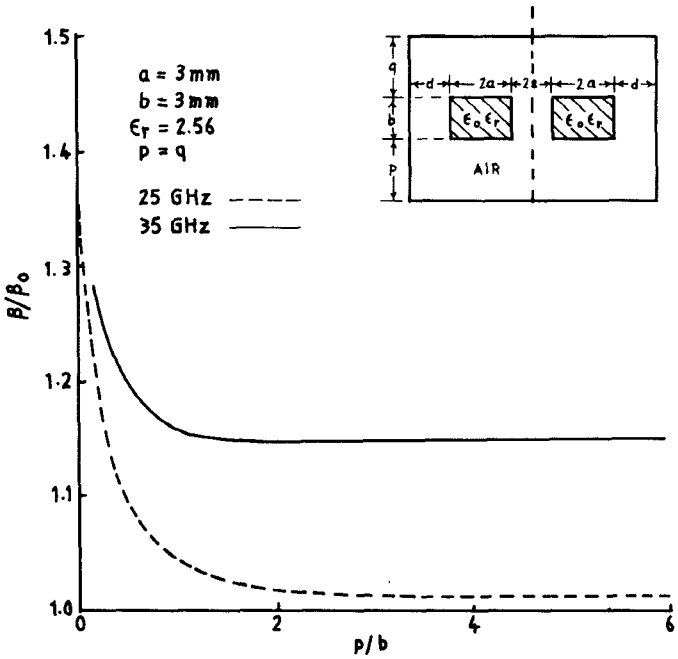

Fig. 3. Variation of β/β_0 with p/b of generalized dielectric waveguide structure for the E_{11}^y mode, $S \to \infty$, $d \to \infty$.

This procedure is already reported by several authors [4], [6], [13], [14].

Fig. 3 shows a typical plot of normalized propagation constant β/β_0 as a function of p/b ($q = p$) at two frequencies, namely, 25 and 35 GHz for $M = 2$, where M is the summation number defined in the Appendix. It is apparent from the figure that top and bottom metal planes have negligible effect on β/β_0 for $p/b \geqslant 2$. Hence, in all subsequent computations of β/β_0 where the effect of top and bottom metal planes has to be ignored, p/b is assumed to be $\geqslant 2$, and $M = 2$.

III. Reduction of Generalized Dielectric Guide to Other Dielectric Guide Structures

The various single guide structures which will be obtained as special cases of the generalized coupled dielectric guide structure for odd-mode excitations are listed below:

1) shielded rectangular dielectric guide, $p = q$ small ($p/b < 2$) and $s = d$ small;
2) trapped insulated image guide, p small ($p/b < 1$), q large ($q/b \geqslant 2$), and $s = d$ small;
3) trapped image guide, $p = 0$, q large ($q/b \geqslant 2$), and $s = d$ small; and
4) insulated nonradiative guide, $p = q$ large ($p/b \geqslant 2$), $s = d$ small, and high ϵ_r of the dielectric slab.

The various coupled dielectric guide structures which will be obtained as special cases of the generalized coupled dielectric guide structure are listed below:

1) shielded suspended coupled dielectric guide, $p = q$ small ($p/b < 2$), and $s = d$ small;
2) trapped coupled insulated image guide, p small ($p/b < 1$), q large ($p/b \geqslant 2$), and $s = d$ small;

3) trapped coupled dielectric image guide $p = 0$, q large ($p/b \geq 2$), and $s = d$ small;
4) insulated nonradiative coupled dielectric guide, $p = q$ large ($p/b \geq 2$), $s = d$ small, and high ϵ_r of dielectric slabs;
5) nonradiative coupled dielectric image guide, $p = q$ large, ($p/b \geq 2$), $s = d$, and high ϵ_r of dielectric slabs;
6) insulated broadside coupled dielectric guide, $p = q$ large ($p/b \geq 2$), $s = d$ small, and low ϵ_r of dielectric slabs; and
7) broadside coupled dielectric image guide, $p = q$ large ($p/b \geq 2$), $d = 0$, and low ϵ_r of dielectric slabs.

IV. Discussion

A. Shielded Suspended Dielectric Guide

Fig. 4 shows the variation of normalized propagation constant β/β_0 with frequency for shielded suspended dielectric guide having dielectric slab aspect ratios of 0.5 and 1.0. The dielectric materials used are polystyrene ($\epsilon_r = 2.56$) and stycast ($\epsilon_r = 3.4$). The dimensions A and B of the shielding enclosure are 7.112 and 3.55 mm, respectively, for the *Ka*-band waveguide. It is observed that for a fixed value of $b/2q$, β/β_0 is higher for higher values of ϵ_r. Further, the frequency corresponding to $\beta/\beta_0 = 0$ is reduced with an increase in ϵ_r of the dielectric slab. For $\beta/\beta_0 < 1$, the shielded suspended dielectric guide operates in the waveguide mode, while for $\beta/\beta_0 > 1$ it operates in the image guide mode.

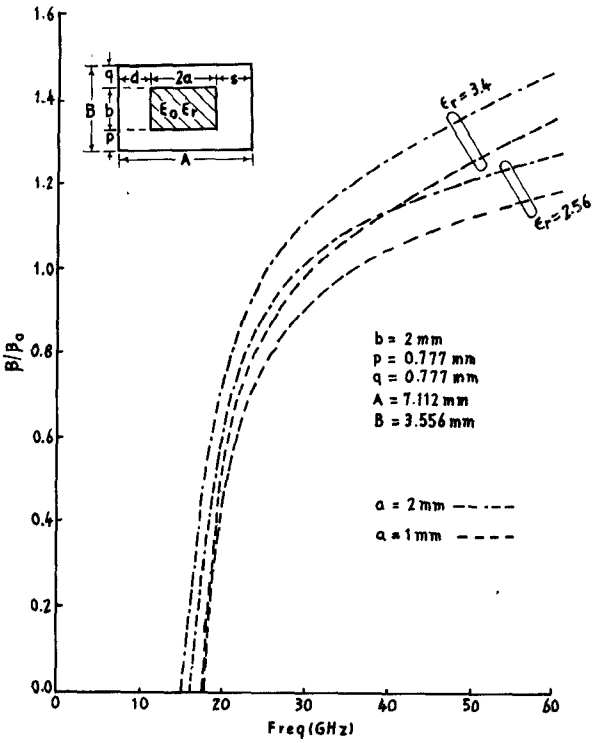

Fig. 4. Variation of β/β_0 with frequency of shielded rectangular dielectric guide with aspect ratios $b/2a = 0.5$ and 1.0 with dielectric polystyrene and stycast.

B. Trapped Insulated Image Guide

The effect of the bottom metallic plane on the normalized propagation characteristics is shown in Fig. 5. The top metal plane distance is kept at 6 mm, so that it has a negligible effect on the propagation. It is seen that, for a fixed frequency, β/β_0 decreases with an increase in the insulating layer thickness. Further, with all other parameters fixed, the cutoff frequency corresponding to $\beta/\beta_0 = 1$ increases with an increase in the insulating layer thickness.

C. Trapped Image Guide

In Fig. 5, the curve for $p = 0$ shows the variation of β/β_0 with frequency of a trapped image guide. It is apparent from the curves that, keeping all dimensional parameters the same, the cutoff frequency of the insulated trapped image guide is higher compared to that of the trapped image guide. Further, due to an air gap near the image plane, the conductor loss of the trapped insulated image guide will be less compared to that of the trapped image guide.

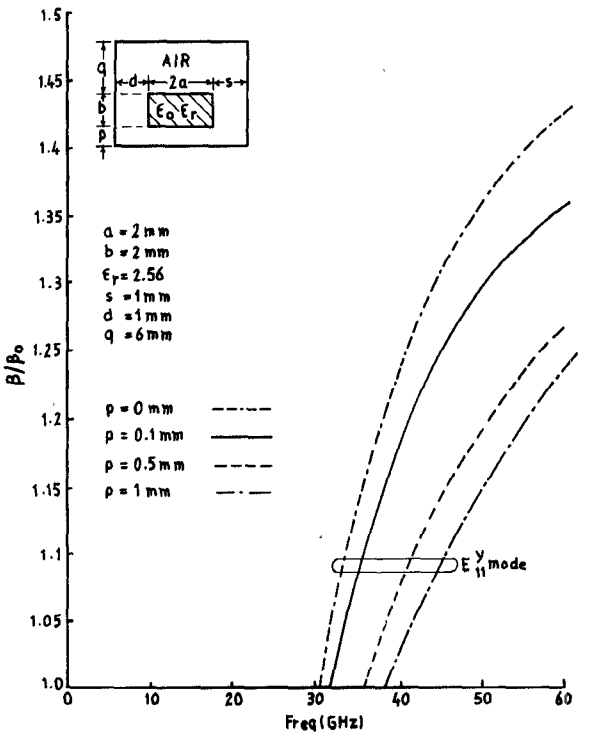

Fig. 5. Variation of β/β_0 with frequency of insular image guide for various insulating layer thicknesses.

D. Insulated Nonradiative Guide

In Fig. 1, if we keep $p = q$ ($p/b > 2$), the side wall distance d and half-spacing s sufficiently small and ϵ_R higher, in odd-mode excitation the structure works as an insulated nonradiative dielectric guide. This guide was proposed by Yoneyama *et al.* using the effective dielectric constant method [15]. However, analysis of this guide using the mode-matching technique has not been reported. The structure reduces to a nonradiative guide when $s = d$

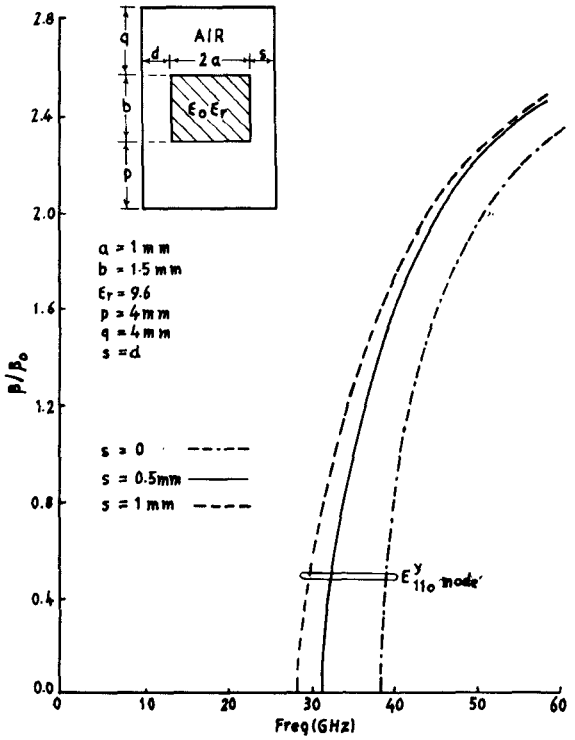

Fig. 6. Variation of β/β_0 with frequency of insulated nonradiative dielectric waveguide.

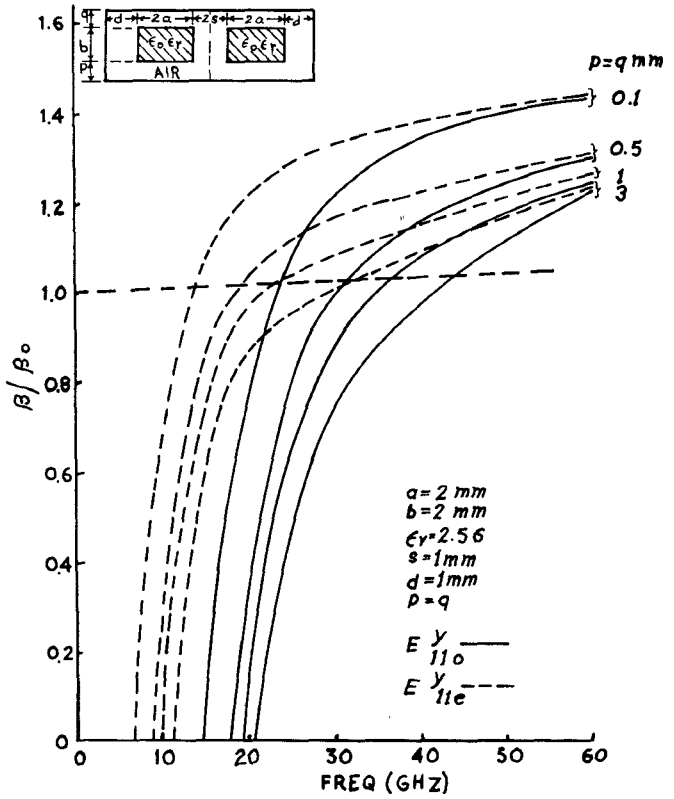

Fig. 7. Variation of β/β_0 with frequency of shielded suspended coupled dielectric guide for various values of p.

$= 0$ [12]. Fig. 6 shows the variation of β/β_0 with frequency for an insulated nonradiative guide. The half-spacing s is kept equal to d. For the parameters chosen, the dielectric guide is nonradiative since the cutoff frequencies of the parallel plate TM mode for $s = 0$, 0.5, and 1 mm are 75, 50, and 37.5 GHz, respectively, while the cutoff frequencies of the dielectric guide corresponding to β/β_0 for $s = 0$, 0.5, and 1 mm occur at 38, 32, and 27.9 GHz, respectively.

E. Shielded Suspended Coupled Dielectric Guide

If the distance q of the top metal plane and distance p of the bottom metal plane are very small, the electromagnetic field distribution inside the generalized coupled dielectric guide is modified, and consequently, β/β_0 also changes. Fig. 7 shows the variation of β/β_0 as a function of frequency for various values of p such that $p/b < 2$. The distance q is taken equal to p so that the structure is symmetric. Since all the four shielding walls are sufficiently close to the dielectric slab, the structure is designated as a shielded suspended coupled dielectric guide. The characteristics shown in Fig. 7 are for the structure having dielectric slabs with aspect ratio $b/2a = 0.5$ and $\epsilon_r = 2.56$. The values of s and d are kept constant ($s = 1$ mm). It is observed that with $p = q$ and for fixed frequency, as the distance p is increased, β/β_0 decreases for both even and odd modes. Further, with an increase in p, the cutoff frequencies for the even and odd modes increase.

F. Insulated Broadside Coupled Dielectric Guide

The generalized coupled dielectric guide can be represented by an insulated broadside coupled dielectric guide where the insulating layer thickness in the spacing d is air.

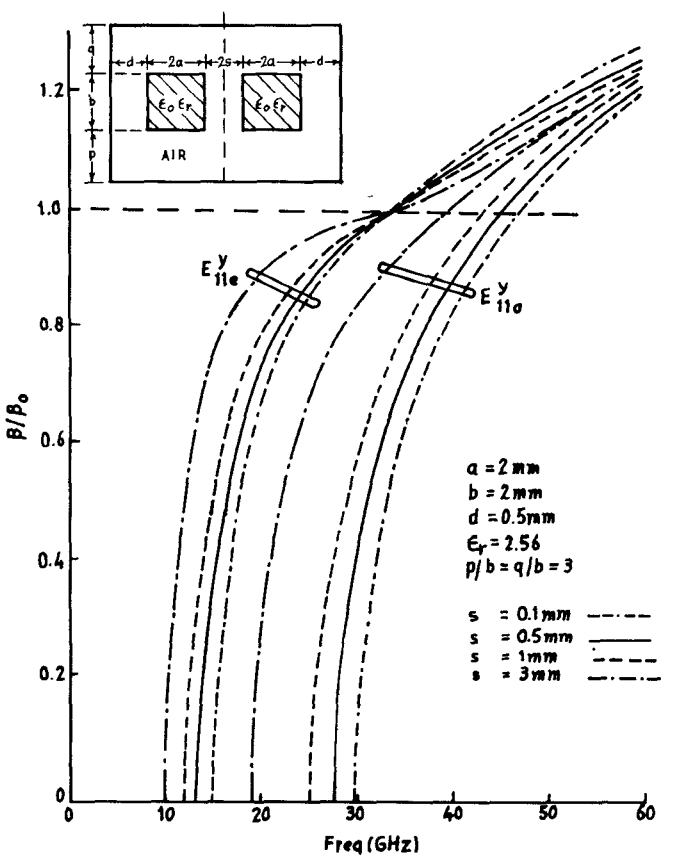

Fig. 8. Variation of β/β_0 with frequency of insulated broadside coupled dielectric guide.

The variation of β/β_0 with frequency for E^y_{11e} and E^y_{11o} modes of the insulated broadside coupled dielectric guide are shown in Fig. 8. The half-spacing s between the two dielectric slabs is the variable parameter. From Fig. 8, it is observed that in the case of even modes, the dispersion curves for various values of s cross each other at $\beta/\beta_0 = 1$. Further, for a given frequency, with an increase in half-spacing s, β/β_0 decreases in the range $\beta/\beta_0 > 1$ and increases with s in the region $\beta/\beta_0 < 1$. For both even and odd modes, the cutoff frequency corresponding to $\beta/\beta_0 = 0$ decreases with an increase in s.

G. Broadside Coupled Dielectric Guide

In the insulated broadside-coupled dielectric guide, if the insulating layer (air in this case as dielectric) thickness d is set equal to zero, the structure reduces to a broadside-coupled dielectric guide. Although the conductor loss in the broadside-coupled dielectric guide will be higher compared to the insulated broadside-coupled dielectric guide, it will be much lower than that of the edge-coupled dielectric image guide with the same aspect ratio. The dispersion characteristics of this guide are reported by the authors elsewhere [13].

H. Insulated Nonradiative Coupled Dielectric Guide

In order to use the insulated broadside-coupled dielectric guide as an insulated nonradiative coupled dielectric guide, the dielectric constant of the guiding slabs should be sufficiently high. Fig. 9 shows the variation of the normalized propagation constant β/β_0 with frequency. The dielectric is alumina with $\epsilon_r = 9.6$. It is observed from the figure that the cutoff frequencies of the dominant odd mode for $s = 0.1$, 0.5, and 1 mm are 24, 23.2, and 22.9 GHz, respectively, whereas the cutoff frequencies of the TM parallel plate mode for $s = 0.1$, 0.5, and 1 mm are 28.8, 25, and 21.44 GHz, respectively. Hence, it is obvious that for values $s = 0.1$ and 0.5 mm, the coupled dielectric guide will operate in the nonradiative mode, while for $s = 1$ mm and above, the guide will be operated in the image guide mode region.

I. Nonradiative Coupled Dielectric Image Guide

In the insulated nonradiative coupled dielectric guide, if the distance d of the side walls is kept equal to zero, the structure reduces to a nonradiative coupled dielectric image guide. The dispersion characteristics of this dielectric guide are already reported by the authors elsewhere [14].

J. Coupled Trapped Insulated Image Guide

The coupled insulated image guide without side walls has been reported by McLevige *et al.* [3]. However, effects of side walls on the propagation parameters have not been studied. In Fig. 1, if the distance p is reduced to a small value and the distance q is increased to a large value ($q/b \geq 2$), so that the top metallic wall has a negligible effect on the field distribution, the structure reduces to the coupled trapped insulated image guide. In view of the air gap between the dielectric slab and the bottom ground plane, most of the electromagnetic energy will be confined to the dielectric slab, thus keeping the ground plane conductor loss low. Additional conductor loss will be introduced by the side walls, but the contribution due to these is rather small compared to that due to the bottom ground plane.

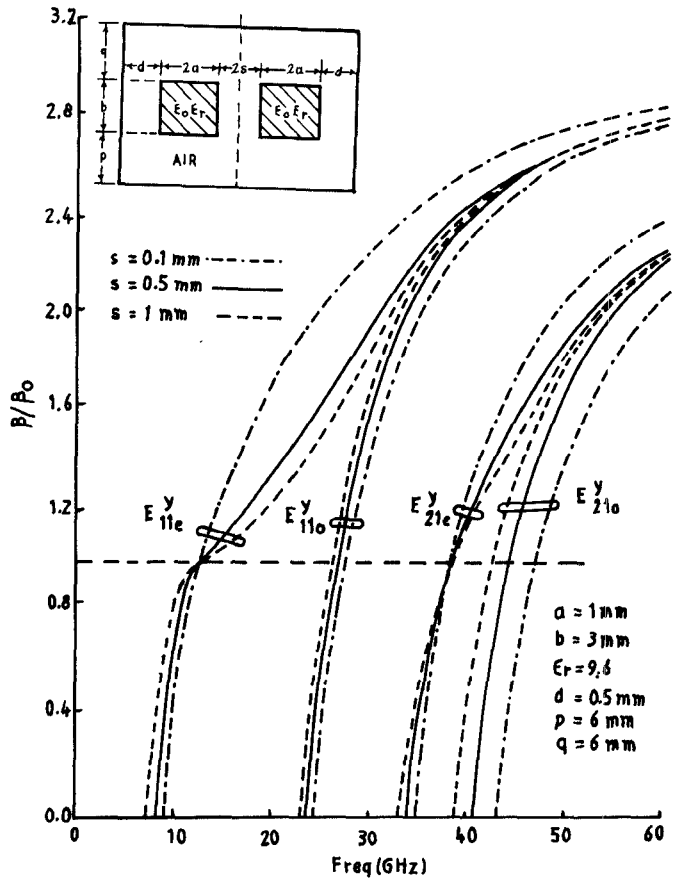

Fig. 9. Variation of β/β_0 with frequency of the insulated nonradiative dielectric guide with alumina dielectric.

Fig. 10 shows the dispersion characteristics for even and odd modes of the above guide, the insulating layer thickness p being a variable parameter. It is apparent from the figure that as the insulating layer thickness p is increased the normalized propagation constant of even and odd modes decreases for a given frequency. The frequency corresponding to $\beta/\beta_0 = 1$ for even and odd modes, and also the separation between these two frequencies, increases with an increase in insulating layer thickness. The reason for this behavior is that as the insulating layer thickness is increased the effective dielectric constant of the structure is reduced, and thus the normalized propagation constant decreases and the frequency corresponding to $\beta/\beta_0 = 1$ increases.

K. Trapped Coupled Dielectric Image Guide

In the coupled trapped insulated image guide structure, if we set $p = 0$, the structure reduces to the trapped coupled dielectric image guide. The dispersion characteristics of this guide have already been reported by the authors elsewhere [12].

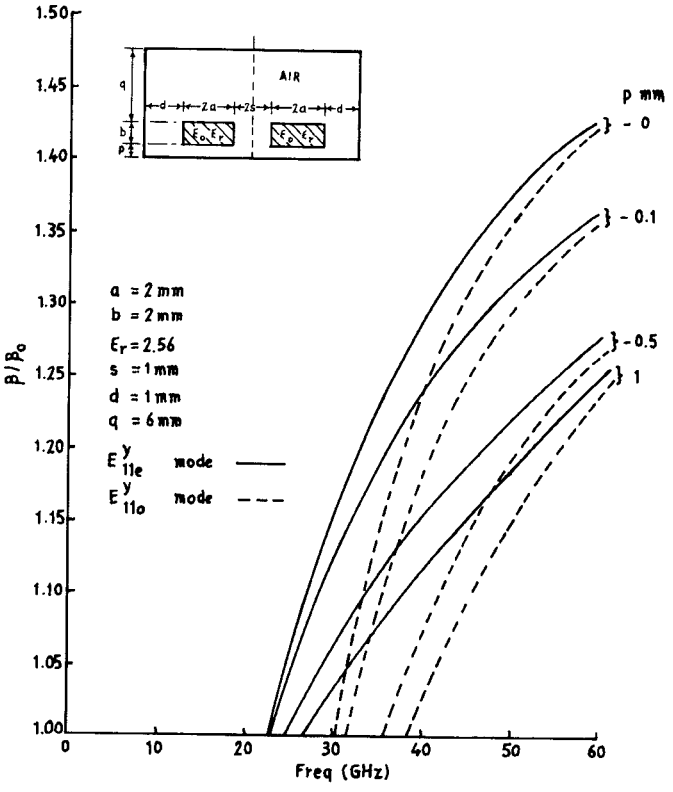

Fig. 10. Variation of β/β_0 with frequency of coupled trapped insulated image guide for various insulating layer thicknesses with polystyrene dielectric.

V. Conclusions

In this paper, a generalized coupled dielectric guide configuration has been considered, and a number of single and coupled dielectric guides are obtained as its variants by using appropriate parameters and dielectric constants, using only one computation formula. The low-loss coupled dielectric guides such as the insulated broadside-coupled dielectric guide, broadside-coupled dielectric guide, shielded suspended, coupled dielectric guide, and insulated trapped coupled dielectric guide will be very useful for construction of couplers in traveling-wave configurations.

Appendix

TM Mode

The scalar potential functions of the mth mode in different regions are given by the following.

Region I:

$$f^e_{1m}(x,y)=\sum_{m=1}^{M}\left[A_m\cos(\beta_{1ym}y)\sin\{\beta_{1xm}(x+d+a)\}\right],$$
$$0\leqslant y\leqslant p+b+q). \quad (1)$$

Region II:

$$f^e_{2m}(x,y)=\sum_{m=1}^{M}\left[\{(B_m\cos(\beta_{2xm}x)+B'_m\sin(\beta_{2xm}x)\}\cdot\{\cos\beta_{2ym}\{y-(p+b+q)\}\}\right],$$
$$p+b\leqslant y\leqslant p+b+q. \quad (2)$$

Region III:

$$f^e_{3m}(x,y)=\sum_{m=1}^{M}\left[\{C_m\cos(\beta_{3xm}x)+c'm\sin(\beta_{3xm}x)\}\cdot\{F_m\cos\beta_{3ym}(y-p)+F'_m\sin\{\beta_{3ym}(y-p)\}\}\right],$$
$$p\leqslant y\leqslant p+b. \quad (3)$$

Region IV:

$$f^e_{4m}(x,y)=\sum_{m=1}^{M}\left[\{D_m\cos(\beta_{4xm}x)+D'_m\sin(\beta_{4xm}x)\}\cdot\{\cos(\beta_{4ym}y)\}\right],\qquad 0\leqslant y\leqslant p. \quad (4)$$

Region V: Magnetic wall at $x=s+a$:

$$f^e_{5m}(x,y)=\sum_{m=0}^{M}\left[E_m\cos(\beta_{5ym}y)\cos\{\beta_{5xm}(x-s-a)\}\right],$$
$$0\leqslant y\leqslant p+b+q. \quad (5)$$

Electric wall at $x=s+a$:

$$f^e_{5m}(x,y)=\sum_{m=0}^{M}E_m\cos(\beta_{5ym}y)\sin\{\beta_{5xm}(x-s-a)\}\Big],$$
$$0\leqslant y\leqslant p+b+q. \quad (6)$$

TE Mode

The potential functions of the nth mode in different regions are given by the following.

Region I:

$$f^h_{1n}(x,y)=\sum_{n=0}^{M}F_n\sin(\bar\beta_{1yn}y)\cos\{\bar\beta_{1xn}(x+d+a)\}\Big],$$
$$0\leqslant y\leqslant p+b+q. \quad (7)$$

Region II:

$$f^h_{2n}(x,y)=\sum_{n=1}^{N}\left[\{G_n\cos(\bar\beta_{2xn}x)+G'_n\sin(\bar\beta_{2xn}x)\}\cdot\sin\left[\bar\beta_{2yn}\{y-(p+b+q)\}\right]\right],$$
$$p+b\leqslant y\leqslant p+b+q. \quad (8)$$

Region III:

$$f^h_{3n}(x,y)=\sum_{n=1}^{N}\left[\{H_n\cos(\bar\beta_{3xn}x)+H'_n\sin(\bar\beta_{3xn}x)\}\cdot\{K_n\cos\{\bar\beta_{3yn}(y-p)\}+K'_n\sin\{\bar\beta_{3yn}(y-p)\}\}\right],$$
$$p\leqslant y\leqslant p+b. \quad (9)$$

Region IV:

$$f^h_{4n}(x,y)=\sum_{n=1}^{N}\left[\{J_n\cos(\bar\beta_{4xn}x)+J'_n\sin(\bar\beta_{4xn}x)\}\cdot\sin(\bar\beta_{4yn}y)\right],\qquad 0\leqslant y\leqslant p+b+q. \quad (10)$$

Region V: Magnetic wall at $x = s + a$:

$$f_{5n}^{h}(x, y) = \sum_{n=0}^{N} \left\{ L_n \sin\left(\bar{\beta}_{5yn} y\right) \sin\left\{ \bar{\beta}_{5xn}(x - s - a) \right\} \right\},$$
$$0 \leqslant y \leqslant p + b + q. \quad (11)$$

Electric wall at $x = s + a$:

$$f_{5n}^{h}(x, y) = \sum_{n=0}^{N} L_n \cos\left\{ \bar{\beta}_{5xn}(x - s - a) \sin\left(\bar{\beta}_{5yn} y\right) \right\},$$
$$0 \leqslant y \leqslant p + b + q. \quad (12)$$

References

[1] E. A. J. Marcatili, "Dielectric rectangular waveguide and directional couplers for integrated optics," *Bell Syst. Tech. J.*, vol. 48, pp. 2071–2102, Sept. 1969.

[2] R. M. Knox and P. P. Toulios, "Integrated circuits for the millimeter through optical frequency range," in *Proc. Symp. Submillimeter Waves*, New York, Mar. 31–Apr. 2, 1970, pp. 497–515.

[3] M. V. McLevige, T. Itoh, and R. Mittra, "New waveguide structures for millimeter wave and optical integrated circuits," *IEEE Trans. Microwave Theory Tech.*, vol. MTT-23, pp. 788–794, Oct. 1975.

[4] R. Mittra, "Analysis of open dielectric waveguides using mode matching technique and variational methods," *IEEE Trans. Microwave Theory Tech.*, vol. MTT-28, pp. 36–43, Jan. 1980.

[5] M. Dydyk, "Image guide: A promising medium for EHP circuits," *Microwaves*, pp. 71–80, Apr. 1981.

[6] K. Solbach and I. Wolff, "The electromagnetic fields and the phase constant of dielectric image lines," *IEEE Trans. Microwave Theory Tech.*, vol. MTT-26, pp. 266–274, Apr. 1978.

[7] P. P. Toulios, "Image line millimeter integrated circuits directional coupler design," in *Proc. Nat. Electron. Conf.*, Chicago, IL, Dec. 1970, pp. 645–650.

[8] S. Shindo and T. Itanami, "Low loss dielectric image line for millimeter wave integrated circuits," *IEEE Trans. Microwave Theory Tech.*, vol. MTT-26, 747–751, Oct. 1978.

[9] T. Itoh and B. Adelseck, "Trapped image guide for millimeter wave circuits," *IEEE Trans. Microwave Theory Tech.*, vol. MTT-28, pp. 1433–1436, Dec. 1980.

[10] T. N. Trinh and R. Mitra, "Suspended *H* guide and its millimeter wave applications," in *1983 Int. Microwave Symp. Dig.*

[11] W. Schlosser and H. G. Unger, "Partially filled wave guides and surface wave guides of rectangular cross section," in *Advances in Microwaves*. New York: Academic, 1966, pp. 319–387.

[12] T. Yoneyama and S. Nishida, "Nonradiative dielectric wave guide for millimeter wave integrated circuits," *IEEE Trans. Microwave Tech.*, vol. MTT-29, pp. 1188–1192.

[13] A. K. Tiwari and B. Bhat, "Analysis of trapped single and coupled image guides using the mode matching technique," *AEU Band 38*, pp. 181–185, May/June 1984.

[14] B. Bhat and A. K. Tiwari, "Analysis of low loss broadside coupled dielectric image guide using the mode matching technique," *IEEE Trans. Microwave Theory Tech.*, vol. MTT-32, pp. 711–716, July 1984.

[15] T. Yoneyama, S. Fujita, and S. Nishida, "Insulated nonradiative dielectric waveguide for millimeter wave integrated circuits," in *IEEE Microwave Theory Tech. Symp.*, June 1–3, 1983, p. 13.

[16] R. F. Harrington, *Time-Harmonic Electromagnetic Fields*. New York: McGraw-Hill, 1961.

A. K. Tiwari was born in Jabalpur, India, on January 4, 1947. He received the B.Sc, B.E.Sc, and M.E degrees from the University of Jabalpur and the Ph.D degree from the Indian Institute of Technology, New Delhi.

From 1972 to 1974 he worked for the Border Security Force for development of miniaturized V.H.F. transmitters, and since 1975 he has been working in the Department of Electronics, Maulana Azad College of Technology, Bhopal, India. He is currently engaged in the design and development of dielectric image guide antennas and the nonradiative coupled dielectric guide.

Dr. Tiwari has published a number of papers in the IEEE TRANSACTIONS ON MICROWAVE THEORY AND TECHNIQUES and the *Journal of Infrared and Millimeter Waves*.

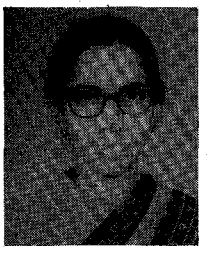

Bharathi Bhat (SM'82) received the B.E. degree in electrical communication engineering and the M.E. degree in electronics, both with distinction, from the Indian Institute of Science, Bangalore, India, in 1963 and 1965, respectively. She continued her graduate studies at Harvard University, Cambridge, MA, and received the M.S. and Ph.D. degrees from the Division of Engineering and Applied Physics in 1967 and 1971, respectively.

From 1971 to 1972, she worked as a postdoctoral Research Fellow in the Division of Engineering and Applied Physics, Harvard University. In 1973, she joined the Indian Institute of Technology, New Delhi, as an Assistant Professor. Since 1977, she has been a Professor at the Centre for Applied Research in Electronics (CARE). During the period 1979–1982, she was the Head of CARE, IIT, New Delhi. She is also the leader of the Microwave Group in CARE, and has been directing a number of sponsored research projects in the areas of microwave antennas, electronic phase shifters, and microwave and millimeter-wave integrated circuits and components.

Dr. Bhat is a Fellow of the Institution of Electronics and Telecommunication Engineers (IETE), India. She has been the Honorary Editor of the IETE Journal (electromagnetics section) since January 1981, and a member of the IETE Council since January 1982. She is presently the Chairman of the ED/MTT Chapter of the IEEE India Council.

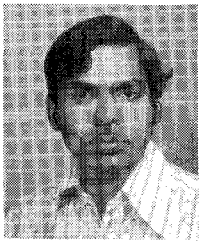

R. P. Singh was born in Nadoya, Varanasi, India, on December 1, 1949. He did graduate and postgraduate work in electronics engineering at the Institute of Technology, Banaras Hindu University, Varanasi, in 1971 and 1973, respectively, and is working for the Ph.D degree from Bhopal University, Bhopal, India.

He is working in the Department of Electronics Engineering, Maulana Azad College of Technology, Bhopal, as a lecturer. His fields of interest are communication systems and microwave engineering.